4176–4184 *Nucleic Acids Research, 1996, Vol. 24, No. 21*

Efficient triple helix formation by oligodeoxyribonucleotides containing α- or β-2-amino-5-(2-deoxy-D-ribofuranosyl) pyridine residues

Paula J. Bates[+], Charles A. Laughton[§], Terence C. Jenkins, Daniel C. Capaldi[1], Peter D. Roselt[1], Colin B. Reese[1] and Stephen Neidle*

The Cancer Research Campaign Biomolecular Structure Unit, The Institute of Cancer Research, Cotswold Road, Sutton, Surrey SM2 5NG, UK and [1]Department of Chemistry, King's College London, The Strand, London WC2R 2LS, UK

Received July 18, 1996; Revised and Accepted September 11, 1996

ABSTRACT

Triple helices containing C^+·G·C triplets are destabilised at physiological pH due to the requirement for base protonation of 2′-deoxycytidine (dC), which has a pK_a of 4.3. The C nucleoside 2-amino-5-(2′-deoxy-β-D-ribofuranosyl)pyridine (β-AP) is structurally analogous to dC but is considerably more basic, with a pK_a of 5.93. We have synthesised 5′-psoralen linked oligodeoxyribonucleotides (ODNs) containing thymidine (dT) and either β-AP or its α-anomer (α-AP) and have assessed their ability to form triplexes with a double-stranded target derived from standard deoxynucleotides (i.e. β-anomers). Third strand ODNs derived from dT and β-AP were found to have considerably higher binding affinities for the target than the corresponding ODNs derived from dT and either dC or 5-methyl-2′-deoxycytidine (5-Me-dC). ODNs containing dT and α-AP also showed enhanced triplex formation with the duplex target and, in addition are more stable in serum-containing medium than standard oligopyrimidine-derived ODNs or ODNs derived from dT and β-AP. Molecular modelling studies showed that an α-anomeric AP nucleotide can be accommodated within an otherwise β-anomeric triplex with only minor perturbation of the triplex structure. Molecular dynamics (MD) simulations on triplexes containing either the α- or β-anomer of (N1-protonated) AP showed that in both cases the base retained two standard hydrogen bonds to its associated guanine when the 'A-type' model of the triplex was used as the start-point for the simulation, but that bifurcated hydrogen bonds resulted when the alternative 'B-type' triplex model was used. The lack of a differential stability between α-AP- and β-AP-containing triplexes at pH >7, predicted from the behaviour of the B-type models, suggests that the A-type models are more appropriate.

INTRODUCTION

Pyrimidine- or purine-rich oligonucleotides can be designed in order to recognise homopurine·homopyrimidine sequences in double-stranded DNA by triple helix (triplex) formation. This approach (the antigene strategy) is seen as a promising method to selectively regulate gene expression (for a review see 1). Triplex-forming oligonucleotides linked to reactive moieties have also been used to introduce covalent modifications which may lead to site-specific cleavage of the target DNA (1–3) or directed mutagenesis (4,5). Triplex formation by purine-rich oligodeoxynucleotides (ODNs) is pH independent, but may be limited by the tendency of guanine-rich ODNs to form competing self-structures (e.g. G tetrads) at physiological ionic strengths (6). ODNs containing G and T may also have biological effects which are not mediated by triplex formation (7,8). Formation of a C^+·G·C triplet (Fig. 1A) requires protonation of the third strand cytosine residues on N3 in order that two Hoogsteen-type hydrogen bonds are formed. Consequently, triplex formation by oligopyrimidines is pH dependent and of relatively low affinity at neutral pH, since the pK_a of dC is 4.3. Triplex stability can be improved by replacing third strand cytosines with 5-methylcytosine residues (5-Me-dC) (9,10). This stabilisation may be partly due to the increased pK_a of 5-Me-dC relative to dC, which leads to more extensive ring protonation at neutral pH, but is thought to result mainly from favourable hydrophobic interactions created by the 'spine' of methyl groups in the major groove (11). A carbocyclic analogue of 5-Me-dC which has a slightly higher pK_a stabilises a triple helix when incorporated into an oligopyrimidine third strand, presumably due to more extensive protonation at the N3 position (12). Nucleoside residues which structurally mimic protonated dC but do not themselves require protonation have also been incorporated into triplex-forming ODNs. These include 2′-deoxyisocytidine (13), 2′-deoxy-8-oxoadenosine and its derivatives (14–16), 2′-deoxy-5-methyl-6-oxocytidine (17), N7-glycosylated guanine (18) and a pyrazole analogue (19). Many of these replacements have led to impres-

*To whom correspondence should be addressed. Tel/Fax: +44 181 643 1675; Email: steve@iris5.icr.ac.uk

Present addresses: [+]Division of Hematology/Oncology, Department of Medicine, The University of Alabama at Birmingham, Birmingham, AL 35294-3300, USA and [§]Department of Pharmaceutical Sciences, University of Nottingham, Nottingham NG7 2RD, UK

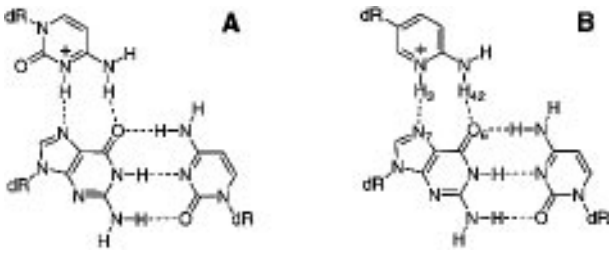

Figure 1. (**A**) Hydrogen bonding scheme for the C^+·G·C base triplet. (**B**) Proposed hydrogen bonding between a protonated AP nucleoside and a G·C base pair.

sive increases in triplex stability at neutral pH, but, with the exception of 5-Me-dC, which gives only a modest improvement in triplex stability, none has been regularly used in antigene studies and the design of such readily synthesised cytosine mimics remains a challenge.

We have designed a C nucleoside analogue, 2-amino-5-(2′-deoxy-β-D-ribofuranosyl)pyridine (β-AP; Fig. 2B), which is a precise structural analogue of dC but has a higher pK_a (5.93 compared with 4.3 for dC). Triplex-forming ODNs containing this nucleoside analogue are expected to have a higher binding affinity for their target at pH 7 compared with the corresponding cytosine-containing ODNs, on the basis that they will be more extensively protonated at neutral pH and are thus able to form two hydrogen bonds to a G·C base pair (Fig. 1B). In this paper we assess the triplex-forming potential of psoralen-derivatised oligonucleotides containing dT and the nucleoside AP. Both the α and β anomers of AP (Fig. 2B and C) have been converted into cyanoethyl phosphoramidites (Fig. 2, I and II). ODNs containing β-dT and β-AP (i.e. a solely β-ODN) or β-dT and α-AP (a mixed α/β-ODN) have been prepared and examined, the latter since α-AP (with a pK_a of 6.16) is a slightly stronger base than β-AP. Because oligonucleotides derived only from α-nucleosides are known to be resistant to nuclease degradation, the stability of the mixed α/β-ODN in serum-containing medium has also been studied. The structure and absolute configuration of a precursor of α-AP have been confirmed by an X-ray crystallographic study (20).

The ODN sequences used in these studies are shown in Figure 3. We have previously demonstrated (21) that a psoralen-linked pyrimidine ODN (Pso-C20) can form a sequence-specific triplex with the duplex AR·AY at pH 7 in the presence of spermine. Previously we have also used psoralen-linked ODNs to form triplex-directed photoadducts with a target in the human aromatase gene (22,23). The target sequence used for this study is similar to that found in the aromatase gene. However, the purine-rich aromatase sequence is interrupted by three pyrimidines and the duplex used here has these bases replaced by purines and thus represents an ‘ideal’ triplex target. In our previous studies photoadduct formation was assessed by a denaturing electrophoretic mobility shift assay, since the crosslinked adduct migrated as a three-stranded species, and any unreacted duplex was denatured and subsequently migrated as the single strands. This method proved to be an easy and reliable way of comparing third strand binding affinities.

There is still considerable uncertainty as to the detailed structure of DNA triplexes and, in particular, as to whether they may be regarded as being more similar to A- or B-type duplex DNA. The original fibre diffraction-based model for the pyrimidine·purine·pyrimidine type triple helix (24,25) had the

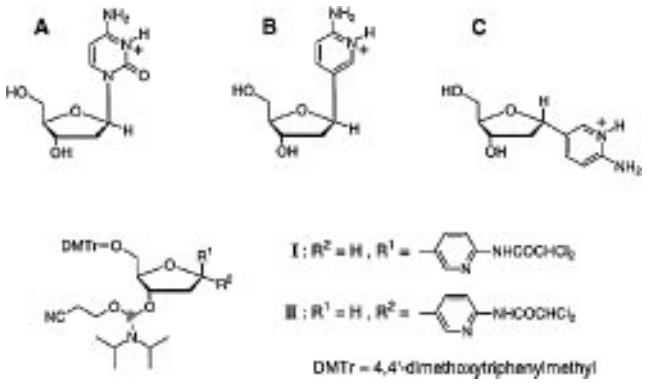

Figure 2. (**A**) Protonated 2′-deoxycytidine in the normal β configuration. 2-Amino-5-(2-deoxy-β-D-ribofuranosyl)pyridine nucleoside (AP) in the (**B**) β- and (**C**) α-anomeric forms. I and II represent respectively the two α- and β-phosphoramidite reagents synthesised.

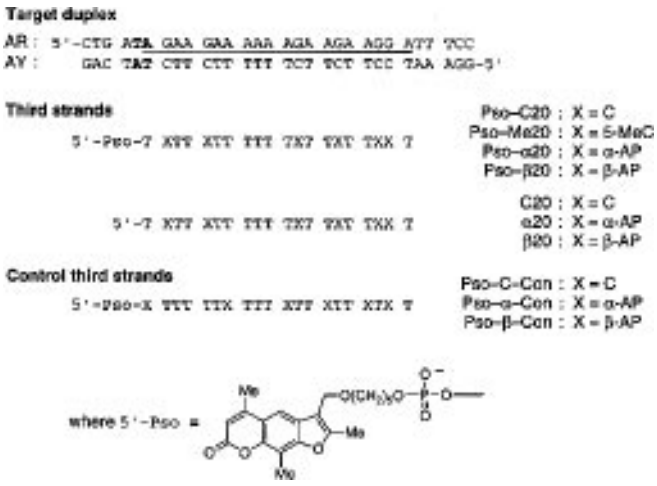

Figure 3. Sequences of oligodeoxynucleotides used. The target homopurine stretch within the synthetic 30mer duplex is shown underlined and the 5′-TpA-3′ step at which the psoralen intercalates is shown in bold. The term Pso-C5 is an abbreviation for 5-[4′-(4,5′,8-trimethylpsoralen)methoxy]pentyl-1-*O*-(2-cyanoethyl)-*N*,*N*-diisopropylphosphoramidite.

large negative *x*-displacement and C3′-*endo* sugar puckers characteristic of A-form duplex DNA. However, more recent NMR studies (26–28) and other spectroscopic studies support a C2′-*endo* sugar pucker, and an alternative B-form model has been postulated as a result (29).

Previous molecular dynamics studies (29–33) have indicated that the conventional ‘A-type’ and ‘B-type’ models for Y·R·Y (pyrimidine·purine·pyrimidine) triplexes probably represent the extremes of an envelope of conformations accessible to these flexible molecules. In this paper we examine the structure and molecular dynamic behaviour of triplexes containing the AP nucleosides, comparing A- and B-type models and the α- and β-anomers of the novel C nucleoside.

MATERIALS AND METHODS

Synthesis and purification of oligonucleotides

Unmodified ODNs were synthesised on an Applied Biosystems 391-EP automated DNA synthesiser using standard phosphor-

amidite chemistry. These ODNs were purified by ion-exchange HPLC and desalted by passage through a Sephadex column. Psoralen-linked ODNs were similarly prepared using a psoralen phosphoramidite, provided as a gift from Dr M.McLean (ICI Diagnostics Ltd) and purified by reversed-phase HPLC.

Oligonucleotides containing modified bases. α-2-Amino-5-(2-deoxy-D-ribofuranosyl)pyridine [α-AP; δ_H[$(CD_3)_2SO$, 360 MHz] 1.72 (1 H, m), 2.41 (1 H, m), 3.41 (1 H, m), 3.49 (1 H, m), 3.75 (1 H, m), 4.16 (1 H, m), 4.69 (1 H, t, *J* 5.7), 4.75 (1 H, dd, *J* 6.5 and 8.9), 5.05 (1 H, d, *J* 4.9), 5.84 (2 H, br s), 6.42 (1 H, d, *J* 8.5), 7.42 (1 H, dd, *J* 2.4 and 8.5), 7.83 (1 H, d, *J* 2.3); δC[$(CD_3)_2SO$, 100.6 MHz] 42.7, 61.6, 71.6, 76.7, 85.8, 107.6, 125.9, 135.5, 145.9, 159.2] and β-2-amino-5-(2-deoxy-D-ribofuranosyl)pyridine [β-AP; δ_H[$(CD_3)_2SO$, 360 MHz] 1.80 (1 H, m), 1.92 (1 H, m), 3.43 (2 H, m), 3.69 (1 H, m), 4.16 (1 H, m), 4.73 (1 H, t, *J* 5.4), 4.82 (1 H, dd, *J* 5.4 and 10.5), 5.01 (1 H, d, *J* 3.7), 5.85 (2 H, br s), 6.40 (1 H, d, *J* 8.5), 7.36 (1 H, dd, *J* 2.1 and 8.4), 7.84 (1 H, d, *J* 2.3); δ_C[$(CD_3)_2SO$, 90.6 MHz] 42.9, 62.5, 72.6, 77.5, 87.5, 108.0, 112.5, 125.1, 136.0, 146.2, 159.5] were prepared from 2-deoxyribose via the corresponding α- and β-2-bromo-5-(2-deoxy-D-ribofuranosyl)pyridines by a novel procedure that is completely unrelated to that recently reported (33). The site of the attachment of the base to the sugar residue and the stereochemistry of the anomeric linkage of α-2-bromo-5-(2-deoxy-D-ribofuranosyl)pyridine were established by an X-ray crystal structure analysis (20). The pK_a values of α- and β-AP were determined spectrometrically (34) in the research laboratories of SmithKline Beecham (Welwyn, UK) and found to be 6.16 and 5.93 respectively. Full details of the preparation of α- and β-AP and the corresponding protected phosphoramidites (II and I respectively) will be published separately. In order to facilitate unblocking of the derived oligonucleotides, the dichloroacetyl group was used to protect the base amino functions of α- and β-AP. Release of the synthetic ODNs from the solid support and removal of the protecting groups was effected by heating with concentrated aqueous ammonia (*d* 0.88, 1.5 ml) at 55°C for 14 h. The ODNs were then purified by reversed-phase HPLC on a Jones APEX ODS 5 µm column (250 × 4.6 mm).

Electrophoretic mobility shift assays

The purine-rich strand (AR) of the target duplex was 5′-end-labelled using [γ-^{32}P]ATP and T4 polynucleotide kinase (New England Biolabs Inc.) and separated from unincorporated ATP by electrophoresis through a 20% polyacrylamide gel. Formation of the duplex (AR·AY) was achieved by mixing radiolabelled AR with an ~5-fold excess of the unlabelled complementary strand (AY) in TAM binding buffer (40 mM Tris–acetate, pH 7.0, 5 mM $MgCl_2$ and 10% w/v sucrose) and heating at 95°C for 5 min followed by slow cooling to room temperature. Radiolabelled duplex (10 000 c.p.m., ~10 fmol/reaction) was then incubated with the third strand oligonucleotide (Pso-C20, Pso-Me20, Pso-β20 or Pso-α20) or an appropriate control oligonucleotide (Pso-C-Con, Pso-α-Con or Pso-β-Con) in TAM binding buffer, pH 7.0, containing 1 mM spermine tetrahydochloride in a total volume of 20 µl. After 1 h, samples were irradiated with long wavelength UV light (366 nm) as previously described (21). Following irradiation, samples were denatured by heating at 95°C for 5 min and resolved by electrophoresis through 16% denaturing polyacrylamide gels containing 7 M urea and 89 mM Tris–borate, 2 mM EDTA buffer, pH 8.3. Gels were visualised by autoradiography and quantified by densitometry using Image Quant software.

Stability of oligonucleotides in serum-containing medium

Oligonucleotides Pso-C20, Pso-α20 and Pso-β20 (140 pmol in 10 µl water) were each added to tubes containing 90 µl Eagle's MEM cell culture medium supplemented with 10% fetal calf serum (FCS). These samples were incubated at 37°C. After times ranging between 15 min and 48 h, an aliqout (10 µl) was removed from each sample and quickly frozen in a dry ice/acetone mixture and stored at –20°C. At the end of the time course, the frozen samples were thawed and analysed by electrophoresis using a 16% denaturing polyacrylamide gel. The gel was visualised by inspection under UV light (254 nm) against a fluorescent background, where the oligonucleotide bands appear as 'shadows'.

The stability of non-psoralenated ODNs was also examined. Oligonucleotides C-20, α-20 and β-20 were 5′-end-labelled with [γ-^{32}P]ATP using T4 polynucleotide kinase and separated from unincorporated ATP. An aliquot of each of these ODNs (100 000 c.p.m., ~100 fmol) was added to 100 µl culture medium supplemented with 10% FCS and incubated at 37°C for various times as described above. The samples were then analysed by denaturing polyacrylamide gel electrophoresis and the resulting gels were visualised by autoradiography.

Molecular modelling

All molecular mechanics (MM) and molecular dynamics (MD) calculations were performed using the AMBER 4.0 program (35) and the standard all-atom parameter set (36), except that phosphate charges were reduced to –0.24 and counterions were omitted (25). A non-bonded cut-off value of 9 Å was used and the dynamics used a 2 fs time step with SHAKE applied to all bonds. Partial charges for AP were calculated using MOPAC/ESP (37) and missing force field parameters were obtained by interpolation from existing parameter values. Visualisation and interactive modelling were performed using the program MidasPlus (38). The 7mer sequences used in the modelling are shown in Figure 4. Initial structures were built by manual alterations to standard A-type and B-type (29,30) triplexes, then energy minimised *in vacuo* using a distant-dependent dielectric constant of $4r_{ij}$ (39).

The A-type model containing α-AP (model αA) was placed in a box of Monte Carlo water with dimensions that ensured that no solute atom was closer than 8.5 Å from a box boundary. The water was minimised, subjected to 10 ps constant pressure dynamics at 100 K and then re-minimised. Position restraints were next used in a minimisation of the whole system to convert the triplex into each of the other models studied, i.e. the B-type model with the α-anomer of AP (αB) and the A-type and B-type models containing the β-anomer of AP (βA and βB). Each model was then subjected to a full energy minimisation to an r.m.s. gradient of 0.1 kcal/mol·Å. This process for construction of the solvated models ensured that each had the same number of water molecules and that the initial solvent distributions were as similar as possible.

For the early stages of the equilibration phase for each model we used a modified version of the Sander module of AMBER that implemented continuously updated restraints. The first and last base triplets were frozen and the rest of the solute restrained to coordinates given by:

$$xc(t + 1) = (1 - \alpha) \cdot xc(t) + \alpha \cdot x(t)$$

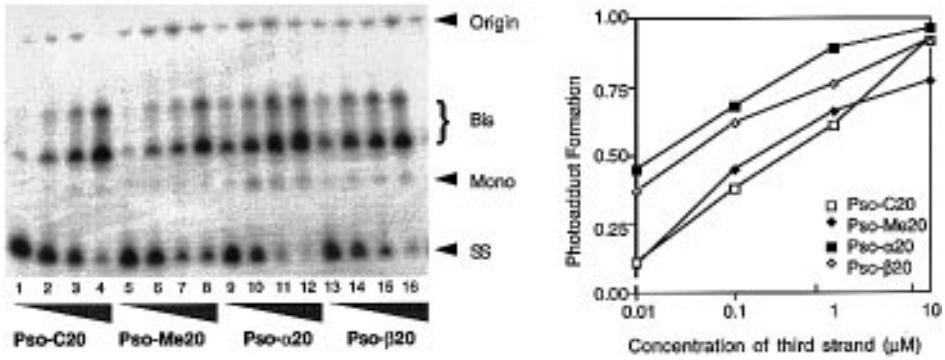

Figure 4. Denaturing electrophoretic mobility shift assay (left) showing triplex-directed photoadduct formation by psoralen-linked oligonucleotides. The concentration of the duplex was ~0.5 nM and of the third strand was 10 (lanes 1, 5, 9 and 13) or 100 nM (lanes 2, 6, 10 and 14) or 1 (lanes 3, 7, 11 and 15) or 10 mM (lanes 4, 8, 12 and 16). These samples were incubated for 1 h at room temperature in TAM buffer, pH 7.0, containing 1 mM spermine. Incubation for longer times (up to 18 h) gave similar results. The graph (right) shows the fraction of photoadduct formation. This was measured as the intensity of the photoadduct bands (bis + mono) divided by the total integrated intensity (i.e. bis + mono + single-stranded bands).

where $xc(t + 1)$ are the restraint coordinates to be used in the next time step and $xc(t)$ those at the current time step, $x(t)$ are the current coordinates and α had a value of 0.1. Using this form of restraint, each model was subjected to 10 ps constant pressure dynamics at 100 K and then 10 ps dynamics at 300 K. Next the restraints were removed (except for the freezing of the first and last base triplets) and each model subjected to 20 ps dynamics at 300 K.

The βA, αB and βB models were well behaved, but in the αA model it was observed that the hydrogen bonding between AP and the guanine had been disrupted, with the formation of a new hydrogen bond between the amino group of AP and N7 of the guanine, while the protonated nitrogen of AP interacted with the nearby phosphate. The protocol for this one simulation was therefore revised. Returning to the structure at the point at which the restraints were first released, the αA model was given 10 ps dynamics at 300 K with restraints to maintain the hydrogen bonding between the AP and guanine bases and then 20 ps free dynamics. This time the model was well behaved. The production phase of the simulation involved a 100 ps constant pressure dynamics run on each model, with the coordinates being saved every 0.5 ps.

RESULTS

Mobility shift assays

In our previous work (22) we have shown that when psoralen-linked triplex-forming ODNs are incubated with their target duplex the psoralen is directed to intercalate at a 5′-TpA-3′ step at the triplex–duplex junction (see Fig. 3). Upon photoactivation with near-UV light (λ > 310 nm), the psoralen forms covalent bonds with the thymine on one strand of the duplex to produce a mono-adduct. Further irradiation allows the covalently bound psoralen to react with the thymine on the opposite strand to form a bis (crosslinked)-adduct. This bis-adduct often appears on a denaturing gel as two bands which increase in parallel (unpublished observations) and we have attributed this to the presence of two species, one of which is incompletely denatured and migrates in the triplex form and another which represents the fully denatured three-stranded species.

Figure 4 shows triplex-directed photoadduct formation by psoralen-linked ODNs containing thymine and either cytosine, 5-methylcytosine, the α-anomer of AP or the β-anomer of AP. The

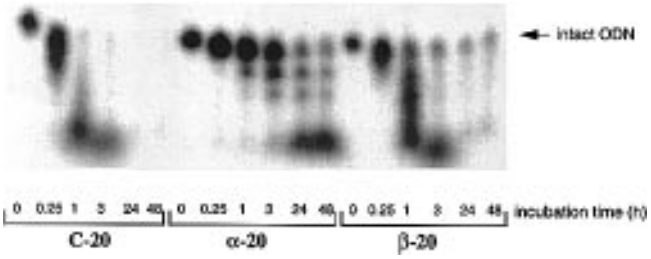

Figure 5. Stability of 5′-radiolabelled ODNs in serum-containing medium following incubation at 37°C for the times shown.

ODNs containing aminopyridine nucleotides (Pso-α20 and Pso-β20) showed a marked increase in affinity for the target relative to the other oligonucleotides examined. Triplex-forming ODNs containing the α-anomeric aminopyridine nucleotides had a slightly higher affinity than those with the β-anomer, possibly due to the increased basicity of the α-anomer (with a pK_a of 6.16) compared with the β-anomer (with a pK_a of 5.93). Both Pso-α20 and Pso-β20 promoted significant photoadduct formation at the lowest third strand concentration used (10 nM), which represents only an ~20-fold excess over the target. Very little adduct formation was detected using the same concentration of the corresponding cytosine- or 5-methylcytosine-containing triplex-forming ODNs.

To ensure that the interaction between the duplex and modified third strands was sequence specific, aliquots of radiolabelled target duplex were incubated with either the matched psoralen-linked ODNs or control psoralen-linked ODNs (see Fig. 2). Samples were then irradiated in parallel and electrophoresed on the same gel. The matched oligonucleotides formed adducts as expected, but no adduct formation was detected with up to 100 μM of the control ODNs (data not shown).

Stability of the oligonucleotides

Figure 5 shows the stability of 5′-radiolabelled oligonucleotides incubated in serum-containing medium. The ODN containing cytosine (C-20) is very quickly degraded, while those containing the non-natural AP nucleoside appear to have a longer lifetime. In particular, the ODN containing the α-anomer of AP appears to have increased resistance to the nucleases present in the medium.

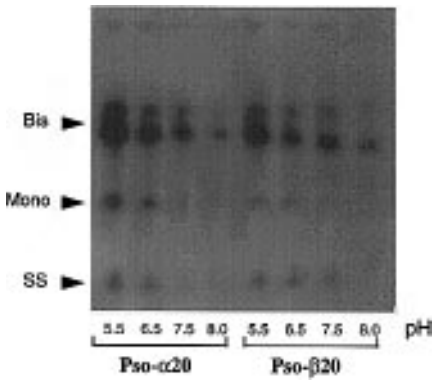

Figure 6. pH dependence of adduct formation. Samples containing the target duplex (10 000 c.p.m./reaction) and 1 μM Pso-α20 or Pso-β20 were incubated overnight in an aqueous buffer containing TAM (40 mM Tris–acetate, 5 mM $MgCl_2$, adjusted to the appropriate pH by addition of acetic acid) and 1 mM spermine. These were then irradiated as described and analysed on a denaturing gel.

After 1 h incubation, ~80% of the radiolabelled species migrates at a similar rate to the intact 20mer. This may represent undegraded 20mer or possibly a 19mer in which the 3′-base (a β-dT) has been removed to leave an α-AP residue at the 3′-terminus. This species is relatively stable and a small amount remains even after 48 h incubation. In contrast to C-20 and β-20, degradation products of the oligonucleotide containing α-AP appear as discrete bands, possibly due to 3′-exonuclease digestion of full-length α-20 to give shorter ODNs with an α-AP nucleoside at the 3′-end. The persistence of a small amount of intact β-20 at longer time points may be due to the formation of secondary structures which confer nuclease resistance.

Comparison of the corresponding psoralen-linked ODNs revealed a similar trend. When fractionated on a denaturing polyacrylamide gel and observed under UV light (254 nm) against a fluorescent background, no intact oligonucleotide was observed at any of the time points examined (i.e. ≥15 min) using either Pso-β20 or Pso-C20, except where the oligonucleotide had been incubated in the absence of serum-containing medium (not shown). Oligonucleotide Pso-α20 was considerably more stable and intact ODN could be observed after 48 h incubation.

pH dependence of triplex formation

Electrophoretic mobility shift assays were carried out to determine the effects of the incubation buffer pH on triplex-directed photoadduct formation by Pso-α20 and Pso-β20. Figure 6 shows that triple helix formation is sensitive to the pH of the incubation buffer, and that triplexes containing either the β- or α-anomer of AP are similarly pH dependent.

Model building with the α-anomer of AP

To our knowledge, there has been no previous report on the effect of including isolated α-anomeric bases within an otherwise all-β triplex-forming ODN on its triplex-forming ability. Somewhat to our surprise, we find that the unnatural anomer α-AP can be introduced into standard models of both A- and B-type triplexes with little structural perturbation. The β-anomer of AP is essentially isostructural with dC itself. The changes required for α-AP are in the ε and ζ torsion angles of the previous (5′) base (from *t* to g^+ and *g*– to g^+ respectively) and in the α torsion of the AP base (from *g*– to *t*). The initial energy minimised structure of model αA is shown in Figure 7.

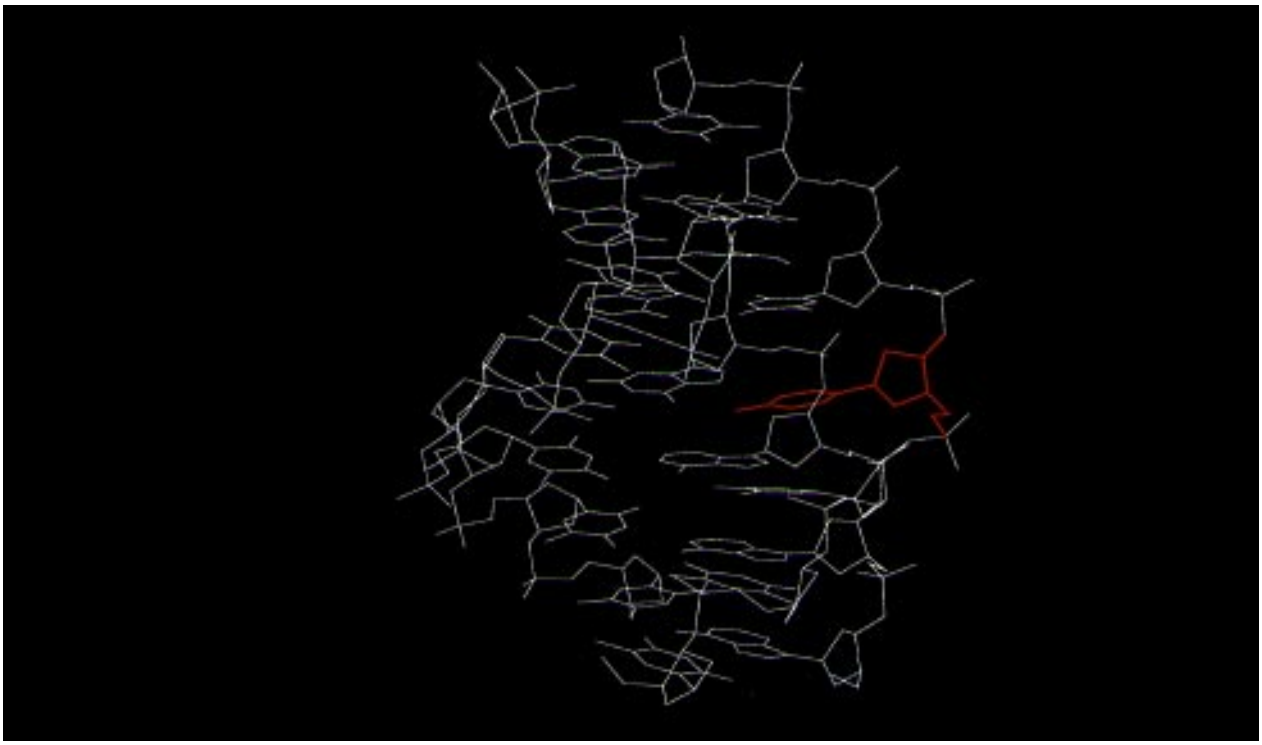

Figure 7. Initial energy minimised structure of model αA. The AP base is shown in red.

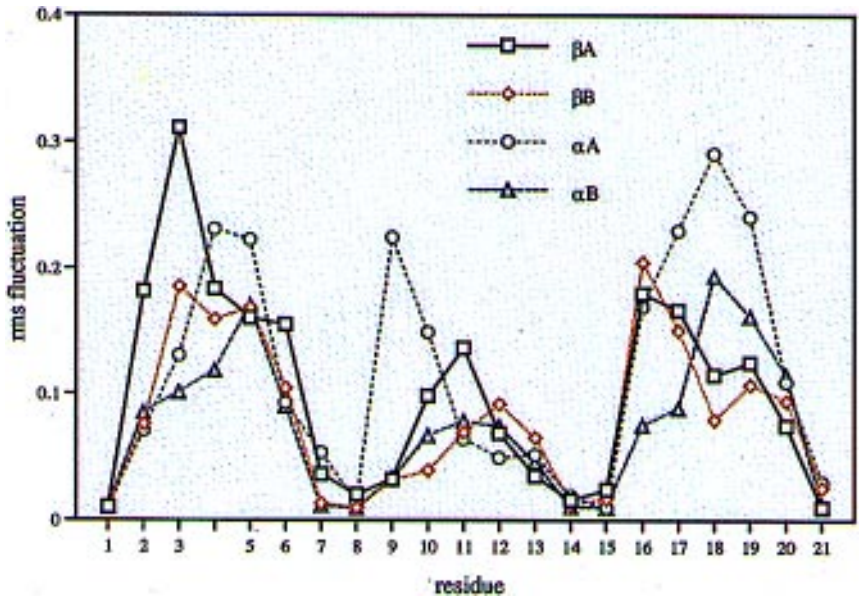

Figure 8. Residue r.m.s. atomic fluctuations from the 100 ps production phase of each MD simulation. Bases 1–7 and 8–14 comprise the Watson–Crick hydrogen bonded pyrimidine and purine strands respectively. Bases 15–21 constitute the AP-containing pyrimidine third strand. The AP base itself is number 18.

Table 1. Average energy components for the last 80 ps of each MD simulation

Component energy term	Model[a]			
	βA	βB	αA	αB
Total	–16228	–16267	–16235	–16269
Potential	–20129	–20140	–20109	–20142
Angle	210	209	213	214
Dihedral	191	178	191	182
1–4 Non-bonded	98	99	98	98
1–4 Electrostatic	–2709	–2721	–2711	–2716
Non-bonded	2352	2346	2358	2347
Electrostatic	–20222	–20201	–20209	–20217
Hydrogen bond	–49	–50	–49	–50

[a]Models refer to α- and β-anomers of the AP nucleotide and the A- and B-type triplex DNA conformations respectively (see text).
Values are in kcal/mol.

Molecular dynamics simulations

Energy component analysis. The average values of the energy components over the last 80 ps of each simulation are shown in Table 1. These are more remarkable for their similarity than for any differences between them, again supporting the notion that the triple helix is a flexible structure. In terms of total potential energy, both α- and β-anomers of AP favour the B-form family of triplex structures. The relative stabilities of the triplexes with the anomers are model dependent; in the A-type simulations the conventional β-anomer of AP gives a lower energy than the α-anomer, but in the B-type simulations the anomers are almost equi-energetic.

DNA flexibility. The residue-averaged values of the atomic coordinate r.m.s. fluctuations over the 100 ps production phase are shown in Figure 8. As expected, the motion of the residues in each strand increases away from the fixed terminal residues. Bases in the oligopyrimidine strands generally show higher r.m.s. fluctuations than those in the oligopurine strand. The AP base shows higher fluctuations in the simulations of the α-anomer triplex than in those of the β-anomer structure, but comparison with the behaviour of the other oligopyrimidine strand shows that in no case does it stand out as being exceptionally mobile.

Time-averaged structures for the AP-containing triplets. The structure of the AP-containing triplet, coordinate-averaged over the last 80 ps of each simulation, is shown in Figure 9. It is evident that for the simulations using the 'A-type' model for the triplex both α- and β-anomers of AP maintain a conformation that preserves the standard triplet hydrogen bonding scheme. The amino group of AP interacts with O6 of guanine and the protonated ring nitrogen of AP with N7 of guanine. For the simulations performed using the 'B-type' triplex model, the results are rather different. For the conventional β-anomer of AP the time-averaged structure shows a hydrogen bond between O6 of guanine and the protonated nitrogen of AP, while the amino group interacts directly only with the solvent. In contrast, for the

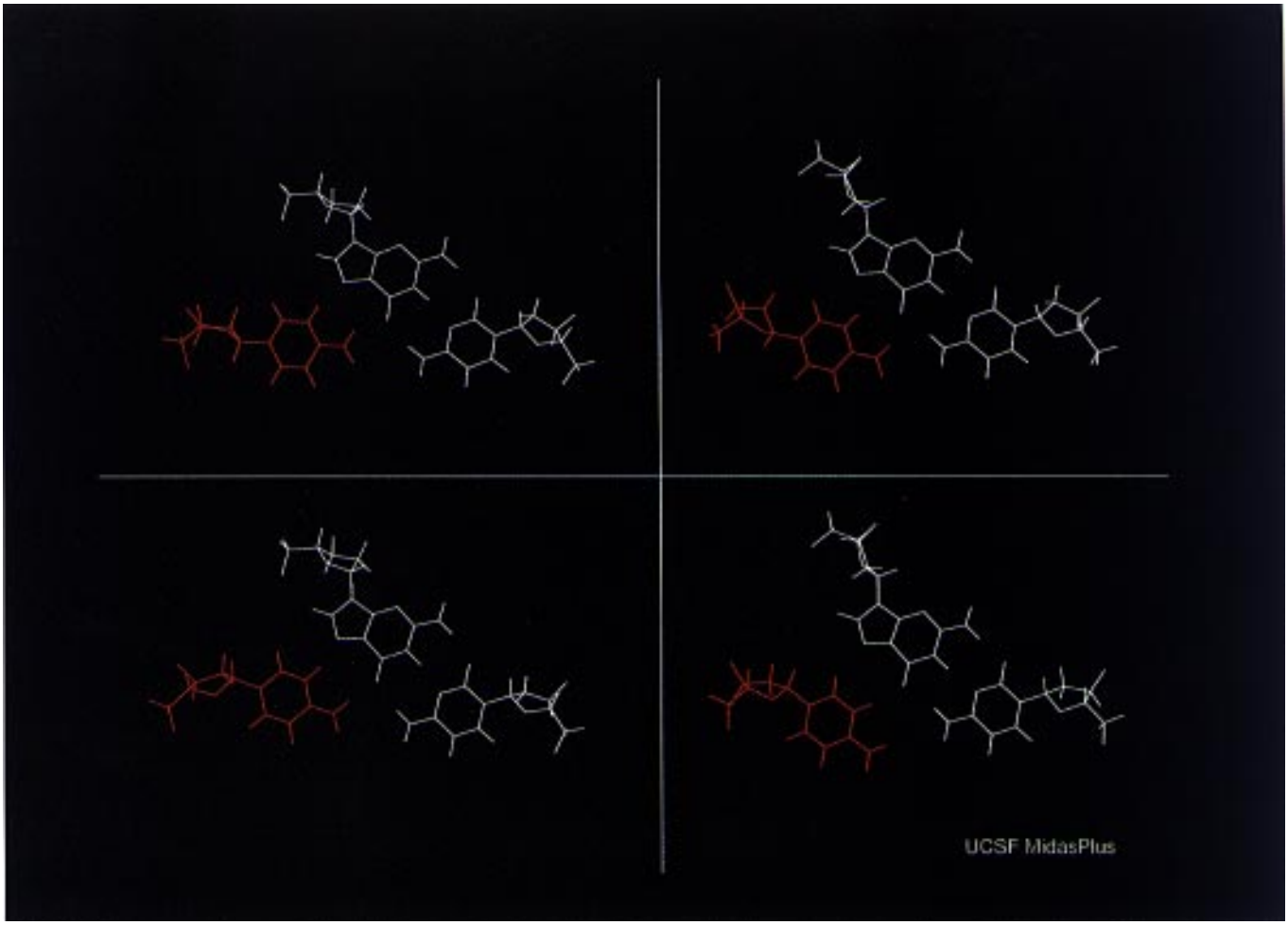

Figure 9. Structures of the AP base triplets, time-averaged over the last 80 ps of each simulation. The AP base is shown in red. Panels are clockwise, from top left: models αA, αB, βA and βB.

α-anomer of AP the amino group interacts with O6 of guanine and the protonated ring nitrogen interacts with both N7 and O6.

Time evolution of the hydrogen bonding pattern. The hydrogen bond donor/acceptor distances for AP and its associated guanine over the last 100 ps of each simulation are plotted in Figure 10. For simulation βA the very stable 'standard' hydrogen bonding pattern is evident, with occasional transient formation of bifurcated hydrogen bonds between N7 of guanine and H42 of AP or O6 of guanine and H3 of AP. For simulation βB the graph shows an initial 40 ps period during which N7 interacts with H3, while O6 is involved in a bifurcated interaction with H42 and H3. Then a conformational transition leads to a situation where only the O6–H3 hydrogen bond is maintained. For simulation αA the 'standard' hydrogen bonding pattern is generally well maintained, with the occasional additional formation of a hydrogen bond between N7 and H42. For simulation αB the N7–H42 interaction is much more evident, although the conventional hydrogen bonds are still usually present.

DISCUSSION

We show here that a 2-aminopyridine nucleoside is a highly effective replacement for deoxycytidine in the third strand of Y·R·Y triple helices. The ability of AP to stabilise this type of triplex at pH 7.0, i.e. close to physiological pH, is markedly superior to 5-methylcytosine, a commonly used replacement for cytosine. As the β-anomer the AP nucleoside is expected to be isostructural with natural dC, thus it is altogether more surprising that the α-anomer of AP is even more effective in stabilising the triplex. Other studies have shown that oligonucleotides containing only α nucleotides are able to form triplexes with β-ODN duplexes that are as stable (in the Y·R·Y motif) or only slightly less stable (G/T third strands) than the corresponding β-ODNs (40). The orientation of these triplex-forming α-ODNs [except where the third strand is oligo(α-dT)], is found to be the opposite of their β-anomeric analogues (36–38). To our knowledge, the results presented here are the first report that a triplex-forming oligonucleotide can contain both α- and β-nucleotides. In contrast to ODNs consisting entirely of α-anomers, this mixed oligonucleotide appears to bind in the same orientation (parallel to the purine strand) as the fully β-anomeric analogue. Previous studies (see for example 39–41) have shown that fully α and chimeric α/β antisense oligonucleotides have marked resistance to nuclease degradation. In this report we have confirmed that the mixed α/β-ODN (Pso-α20) has an increased lifetime in serum-containing medium compared with β oligonucleotides. We have

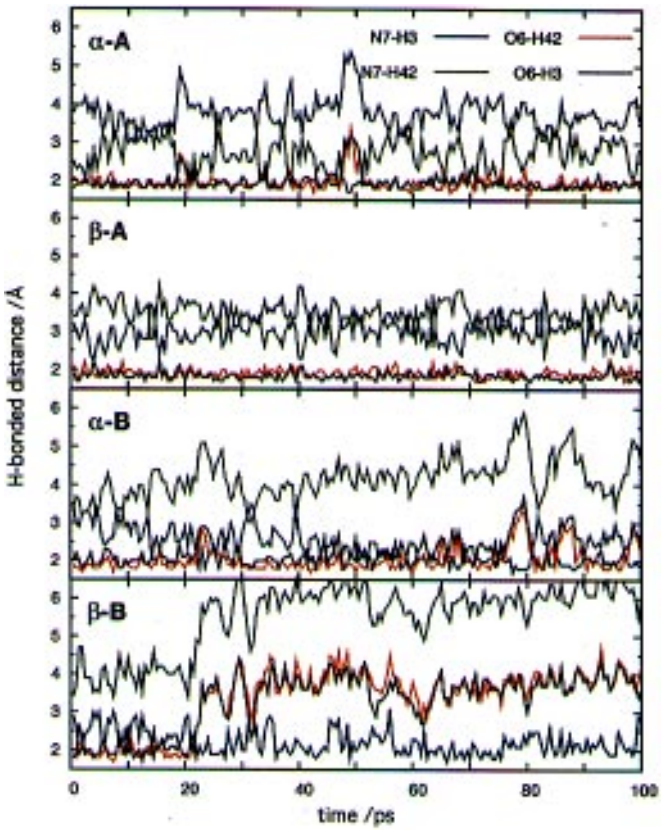

Figure 10. Hydrogen bond distances between AP and its guanine partner during the 100 ps production phase of each simulation (see Fig. 1 for the numbering scheme used). Panels are clockwise, from top left: models αA, αB, βA and βB.

used psoralen-linked oligonucleotides in this study to stabilise triplex formation, since they do not appear to have a significant effect on specificity. Thus the presence of even a single A·C·G or G·C·G triplet virtually abolishes triplex formation; although the weak T·C·G triplet can be tolerated (22) in a psoralen-linked triplex, it greatly reduces its stability.

Oligonucleotides consisting of both α and β nucleosides with either natural (5′–3′) or 3′–3′ and 5′–5′ internucleotide linkages have been studied as potential antisense agents (40,42–45). Whereas α oligonucleotides hydridise readily to their complementary β-strand in a parallel orientation, chimeric α/β-ODNs with short runs of alternating anomers (e.g. a dodecanucleotide consisting of four α nucleotides, followed sequentially by four β nucleotides, then by four α nucleotides) show very poor hybridisation to a complementary β-ODN (40). A mixed triplex-forming α/β-ODN would therefore be unlikely to hybridise to a single-stranded nucleic acid. This property may be advantageous for antigene oligonucleotides, as the possibility of unwanted antisense interactions is reduced.

The pH dependence of the stability of AP-containing triplexes can be used to assess which of the two categories of models for triplex structure, A-type or B-type, is probably more relevant to this particular situation. Models based on the A-type structure (αA and βA) both showed stable ‘standard’ hydrogen bonding between the AP base and its guanine neighbour. Therefore we would predict that triplexes containing either anomer of AP would show a similar pH dependence in their stability. In contrast, models based on the B-type triplex structure (αB and βB) showed differing behaviour in the MD simulations. In model αB hydrogen H42 in AP made the most important hydrogen bonds to its guanine partner, while for model βB it was hydrogen H3 of AP that was most important. As hydrogen H3 is only present in the protonated form of AP, the simulations based on the B-type model therefore predict that triplexes containing the β-anomer of AP should be more pH sensitive than those containing the α-anomer. The experimental results indicate a similar degree of pH sensitivity for both anomers of AP, suggesting that the A-type model of triplex structure is more appropriate, at least for AP-containing triplexes.

During the final stages of the preparation of this manuscript our attention was drawn to synthetic and DNA melting studies of β-AP as a replacement for third strand dC residues by Stefan Hildbrand and Christian Leumann (University of Bern), presented at the International Symposium on Ligands Acting on Nucleic Acids, Switzerland, April 28–May 3, 1996. Their results on enhanced triplex stability parallel our own.

ACKNOWLEDGEMENTS

We are grateful to the Cancer Research Campaign for support with programme and project grants (to SN and CBR respectively). We are grateful to Dr D.Dhanak (SmithKline Beecham, Welwyn) for arranging the pK_a determinations.

REFERENCES

1 Thuong,N.T. and Hélène,C. (1993) *Angew. Chem. Int. Edn English*, **32**, 666–690.
2 Beal,P.A. and Dervan,P.B. (1991) *Science*, **251**, 1360–1363.
3 Strobel,S.A. and Dervan,P.B. (1991) *Nature*, **350**, 172–174.
4 Havre,P.A., Gunther,E.J., Gasparro,F.P. and Glazer,P.M. (1993) *Proc. Natl. Acad. Sci. USA*, **90**, 7879–7883.
5 Wang,G., Levy,D.D., Seidman,M.M. and Glazer,P.M. (1995) *Mol. Cell. Biol.*, **15**, 1759–1768.
6 Olivas,W.M. and Maher,L.J. (1995) *Biochemistry*, **34**, 278–284.
7 Rando,R.F., Ojwang,J., Elbaggari,A., Reyes,G.R., Tinder,R., McGrath,M.S. and Hogan,M.E. (1995) *J. Biol. Chem.*, **270**, 1754–1760.
8 Ojwang,J., Okleberry,K.M., Marshall,H.B., Vu,H.M., Huffman,J.H. and Rando,R.F. (1994) *Antiviral Res.*, **25**, 27–41.
9 Povsic,T.J. and Dervan,P.B. (1989) *J. Am. Chem. Soc.*, **111**, 3059–3061.
10 Sun,J.S., Francois,J.C., Montenay-Garestier,T., Saison-Behmoaras,T., Roig,V., Thuong,N.T. and Hélène,C. (1989) *Proc. Natl. Acad. Sci. USA*, **86**, 9198–9202.
11 Xodo,L.E., Manzini,G., Quadrifoglio,F., van der Marel,G.A. and van Boom,J.H. (1991) *Nucleic Acids Res.*, **19**, 5625–5631.
12 Froehler,B.C. and Ricca,D.J. (1992) *J. Am. Chem. Soc.*, **114**, 8320–8322.
13 Ono,A., T’so,P.O.P. and Kan,L.S. (1992) *J. Org. Chem.*, **57**, 3225–3230.
14 Wang,Q., Tsukahara,S., Yamakawa,H., Takai,K. and Takaku,H. (1994) *FEBS Lett.*, **355**, 11–14.
15 Jetter,M.C. and Hobbs,F.W. (1993) *Biochemistry*, **32**, 3249–3254.
16 Krawczyk,S.H., Milligan,J.F., Wadwani,S., Moulds,C., Froehler,B.C. and Matteucci,M.D. (1992) *Proc. Natl. Acad. Sci. USA*, **89**, 3761–3764.
17 Xiang,G.B., Soussou,W. and McLaughlin,L.W. (1994) *J. Am. Chem. Soc.*, **116**, 11155–11156.
18 Hunziker,J., Priestly,E.S., Brunar,H. and Dervan,P.B. (1995) *J. Am. Chem. Soc.*, **117**, 2661–2662.
19 Koh,J.S. and Dervan,P.B. (1992) *J. Am. Chem. Soc.*, **114**, 1470–1478.
20 Neidle,S., Capaldi,D.C., Joseph,B.V. and Reese,C.B. (1996) *Acta Crystallogr.*, **C52**, 407–409.
21 Bates,P.J., Dosanjh,H.S., Kumar,S., Jenkins,T.C., Laughton,C.A. and Neidle,S. (1995) *Nucleic Acids Res.*, **23**, 3627–3632.
22 Bates,P.J., Macaulay,V.M., McLean,M.J., Jenkins,T.C., Reszka,A.P., Laughton,C.A. and Neidle,S. (1995) *Nucleic Acids Res.*, **23**, 4283–4289.
23 Macaulay,V.M., Bates,P.J., McLean,M.J., Rowlands,M.G., Jenkins,T.C., Ashworth,A. and Neidle,S. (1995) *FEBS Lett.*, **372**, 222–228.

24 Arnott,S and Selsing,E. (1974) *J. Mol. Biol*., **88**, 509–521.
25 Arnott,S., Bond,P.J., Selsing,E. and Smith,P.J.C. (1976) *Nucleic Acids Res*., **3**, 2459–2470.
26 Radhakrishnan,I and Patel,D.J. (1994) *Biochemistry*, **33**, 11405–11416.
27 Radhakrishnan,I., Patel,D.J. and Gao,X. (1992) *Biochemistry*, **144**, 2514–2523.
28 Macaya,R., Wang,E., Schultze,P., Sklenar,V. and Feigon,J. (1992) *J. Mol. Biol*., **225**, 755–773.
29 Raghunathan,G., Miles,H.T. and Sasisekharan,V. (1993) *Biochemistry*, **32**, 455–462.
30 Laughton,C.A. and Neidle,S. (1992) *J. Mol. Biol*., **223**, 519–529.
31 Laughton,C.A. and Neidle,S. (1992) *Nucleic Acids Res*., **20**, 6535–6541.
32 Laughton,C.A. (1995) *Mol. Simulation*, **14**, 275–289.
33 Hsieh,H.-P. and McLaughlin,L.W. (1995) *J. Org. Chem*., **60**, 2356–2359.
34 Albert,A. and Sergeant,E.P. (1992) *Ionisation Constants of Acids and Bases*. Methuen, London, UK, pp. 69–92.
35 Pearlman,D.A., Case,D.A., Caldwell,J.C., Seibel,G.L., Singh,U.C., Weiner,P. and Kollman,P.A. (1991) AMBER 4.0, University of California, San Francisco, CA.
36 Weiner,S.J., Kollman,P.A., Case,D.A., Singh,U.C., Ghio,C., Alagona,G., Profeta,S. and Weiner,P. (1984) *J. Am. Chem. Soc*., **106**, 765–784.
37 Stewart,J.P.P. Mopac 6.0 (QCPE), available from the Quantum Chemistry Programme Exchange, Indiana University, Bloomington, IN.
38 Ferrin,T., Huang,C.C., Jarvis,L.E. and Langridge,R. (1988) *J. Mol. Graphics*, **6**, 13–27.
39 Orozco,M., Laughton,C.A. Herzyk,P. and Neidle,S. (1990) *J. Biomol. Structure Dynam*., **8**, 359–374.
40 Noonberg,S.B., Francois,J.C., Praseuth,D., Guieyssepeugeot,A.L., Lacoste,J., GarestierT. and Hélène,C. (1995) *Nucleic Acids Res*., **23**, 4042–4049.
41 Sun,J.S., Giovannangeli,C., Francois,J.C., Kurfurst,R., Montenay-Garestier,T., Asseline,U., Saison-Behmoaras,T., Thuong,N.T. and Hélène,C. (1991) *Proc. Natl. Acad. Sci. USA*, **88**, 6023–6027.
42 Liquier,J., Letellier,R., Dagneaux,C., Ouali,M., Morvan,F., Rayner,B., Imbach,J.L. and Taillandier,E. (1993) *Biochemistry*, **32**, 10591–10598.
43 Thenet,S., Morvan,F., Bertrand,J.R., Gautie,C. and Malvy,C. (1988) *Biochimie*, **70**, 1729–1732.
44 Debart,F., Tosquellas,G., Rayner,B. and Imbach,J.L. (1994) *Bioorg. Med. Chem. Lett*., **4**, 1041–1046.
45 Vichier-Guerre,S., Pompon,A., Lefebvre,I. and Imbach,J.L. (1994) *Antisense Res. Dev*., **4**, 9–18.
46 Debart,F., Tosquellas,G., Rayner,B. and Imbach,J.L. (1995) *Nucleosides Nucleotides*, **14**, 1015–1018.
47 Boiziau,C., Debart,F., Rayner,B., Imbach,J.L. and Toulme,J.J. (1995) *FEBS Lett*., **361**, 41–45.
48 Koga,M., Moore,M.F. and Beaucage,S.L. (1991) *J. Org. Chem*., **56**, 3757–3759.
49 Neidlein,U. and Leumann,C (1992) *Tetrahedron Lett*., **33**, 8057–8060.